

# Effect of the Slag Composition and a Protective Atmosphere on Chemical Reactions and Non-Metallic Inclusions during Electro-Slag Remelting of a Hot-Work Tool Steel

Reinhold S.E. Schneider,\* Manuel Molnar, Siegfried Gelder, Gerhard Reiter, and Carlos Martinez

The remelting behavior of the hot-work tool steel X37CrMoV5-1 is investigated with several experimental melts on a lab-scale ESR-plant. The investigated parameters comprise a variation of the slag compositions and the use of a protective nitrogen atmosphere. Variations of the slag composition include slags with different contents of  $\text{CaF}_2$ ,  $\text{CaO}$ , and  $\text{Al}_2\text{O}_3$  as well as a variation of the  $\text{SiO}_2$ -content in the slag. The remelted ingots are forged and analyzed regarding their chemical composition. The distribution and composition of the non-metallic inclusions (NMI) is studied by an automated SEM-EDX method. Additionally, the chemical composition of the slag after remelting is analyzed. The results show clearly an equilibrium reaction between Si and Al in the steel with  $\text{SiO}_2$  and  $\text{Al}_2\text{O}_3$  in the slag as well as the effect of oxygen in open ESR operation. A protective atmosphere reduces the Si-losses during remelting, but has no major effect on the number or composition of NMI compared to open remelting. The content of NMI, especially the larger ones, is reduced significantly in all remelting experiments. The majority of the NMI are MA-spinel type except for the CaO-free slag, where alumina inclusions prevail. In general, remelting leads to an almost complete removal of sulfides, a reduction of oxisulfides, and a slight increase of oxides.

inclusions are affected significantly by the remelting slag.<sup>[1,2,6–10]</sup> Furthermore, the slag composition, especially the basicity of the slag, has a major effect on silicon losses.<sup>[1,2,9,11]</sup> Regarding the effect of the slag composition on the composition of the NMI in tool steels after remelting, the existing references are still limited.

The effect of different remelting parameters on the formation of NMI has found renewed interest as a prerequisite for the production of steels with lowest amounts of oxygen and NMI. The effect of a protective atmosphere and additions of a slag deoxidation treatment on a corrosion resistant die steel is described in ref. [5], showing that both measures can provide similar improvements when starting from high oxygen contents in the electrode. On a similar additionally Ni-alloyed grade, higher melt rates resulted in significantly more, but finer NMI and in a corresponding increase of the oxygen content.<sup>[12]</sup> The divergences were attributed to differ-

## 1. Introduction

Like in the early days of electro-slag remelting, as documented, e.g., in refs. [1–3], this process is still mainly used to reduce inhomogeneity (like segregations, shrink holes) and to improve the cleanliness level, especially regarding large non-metallic inclusions (NMI).<sup>[4,5]</sup> The cleanliness level and the type of

ences in the precipitation and growth kinetics. The origin of NMI in a similar steel, determined with a  $\text{La}_2\text{O}_3$ -tracer in the remelting slag, was in the focus of investigations in ref. [13], indicating that, at least for larger inclusions, the majority of NMI are formed newly during solidification, while some  $\text{MgO}\cdot\text{Al}_2\text{O}_3$ -(MA)-spinel type inclusions do either have a too low  $\text{La}_2\text{O}_3$ -solubility or do originate from the electrode. The effect that some inclusions survive from the electrode is additionally supported by results in ref. [14], using different 3D analytical methods, but again with a focus on larger inclusion and remelting of different ingot diameters. Results from industrial trials on hot work tool steels and a martensitic Cr–Ni-steel in ref. [15] demonstrate the strong cleaning effect regarding NMI of ESR, especially of protective gas ESR, almost reaching the quality level of VAR. Most inclusions detected are of the MA-spinel type or have a high  $\text{Al}_2\text{O}_3$ -content. Similar type, but significantly more inclusions were found in a comparable hot-work tool steel from industrial production.<sup>[16]</sup> In this context, the development of NMI over

Prof. R.S.E. Schneider, M. Molnar  
FH-OÖ F&E GmbH  
Stelzhamerstraße 23, 4600 Wels, Austria  
E-mail: r.schneider@fh-wels.at

Dr. S. Gelder, G. Reiter, Dr. C. Martinez  
voestalpine Böhler Edelstahl GmbH & Co KG  
Mariazellerstraße 25, 8605 Kapfenberg, Austria

© 2018 The Authors. Published by WILEY-VCH Verlag GmbH & Co. KGaA, Weinheim. This is an open access article under the terms of the Creative Commons Attribution-NonCommercial License, which permits use, distribution and reproduction in any medium, provided the original work is properly cited and is not used for commercial purposes.

DOI: 10.1002/srin.201800161

the whole process route demonstrates the cleaning effect of the ESR process. The effect of higher SiO<sub>2</sub> additions to the remelting slag on the NMI composition is documented in ref. [17] for a hot work tool steel and confirms earlier results in refs. [1,9] whereby larger inclusions of a mixed (Ca,Al,Mg)O-type with high SiO<sub>2</sub> contents are formed. Nevertheless, and similar to results in ref. [13], the majority of MA-spinels, showed no significant change in composition and are in good agreement with results in ref. [15]. Laboratory scale investigations in ref. [18] with a die steel show advantages of Ar as a protective gas, low filling ratios and a multi-component slag compared to a binary CaF<sub>2</sub>–Al<sub>2</sub>O<sub>3</sub>-slag. Unfortunately detailed information of chemical changes, slag compositions after remelting, and NMI detection methods are missing for better comparison. Substantial effects, both on chemical reactions between the slag and the metal as well as on the NMI composition can be achieved at lower frequency operation due to polarization effects.<sup>[19]</sup> The effect of low frequency ESR in comparison to DC-ESR of both polarities on the number and types of NMI in a similar hot work tool steel is illustrated in ref. [20]. While ESR with DC+ polarity leads to high amounts of Al<sub>2</sub>O<sub>3</sub>-type inclusions in conjunction with strongly increased oxygen contents, MA-spinel type inclusions dominate in 1 Hz AC- and in DC- operation. This effect can be explained by electrochemical reactions similar to ref. [19]. Thereby, it has to be taken into consideration that current densities in ESR operation according to ref. [3] depend highly on the electrode and ingot diameter and the effects found in refs. [19,20] might therefore not be that relevant for large production units. Remelting a high-temperature steel, with high MgO-containing slags lead to stronger reduction of larger NMI with rising MgO-contents up to 10%. In contrast, the number of small inclusions (< 4 μm) increased when the amount of magnesia was raised.<sup>[10]</sup>

With the current work the effects of different slag compositions in the standard system for ESR-slugs (CaF<sub>2</sub>–CaO–Al<sub>2</sub>O<sub>3</sub>), the influence of higher SiO<sub>2</sub>-contents and of a protective N<sub>2</sub>-atmosphere were investigated with the same hot-work tool steel. Thereby, the main focus was on changes in the chemical composition, especially Al, Si, and O during remelting and on corresponding changes in content, size distribution, and chemical composition of particularly small NMI. These results were partially presented in refs. [21,22].

## 2. Experimental Section

All experiments were conducted on a laboratory scale ESR plant with a mold diameter of 165 mm and a low frequency (up to 5 Hz) AC power supply with a maximum current of 5 kA and a maximum voltage of 100 V. A more detailed description on the plant configuration can be found in ref. [23]. To create a protective atmosphere, the mold was covered with a furnace head. Prior to melting operation the atmosphere was blown out by a nitrogen gas stream until the measured oxygen content inside the mold was below 0.1 vol%. The slag was than inserted into the mold by a valve system. During remelting under protective nitrogen atmosphere, a constant gas flow of 30 l min<sup>-1</sup> was applied and the oxygen content was controlled to be ≤0.1 vol%.

### 2.1. Investigated Materials

For the remelting experiments, the hot-work tool steel X37CrMoV5-1 (standard ingot cast and rolled bars) was used. The chemical composition of the steel (electrode) can be taken from Table 3. All electrodes had a diameter of 101.5 mm and a machined metallic bright surface.

A variety of slags was applied to investigate the effect of different slag compositions. The first slag, consisting of roughly one third CaF<sub>2</sub>, one third CaO, and one third Al<sub>2</sub>O<sub>3</sub> can be regarded as a standard-slag in ESR-remelting. This slag was applied twice, once in an open configuration in direct contact with air, and once under protective gas (N<sub>2</sub>). All other experiments were performed only in the open configuration. The standard slag was also enriched with SiO<sub>2</sub> to a starting content of 10% (slag 3C3A1S). Slag 4C4A had a reduced CaF<sub>2</sub>-content and slag 3A was practically free of CaO and MgO. The initial chemical compositions were not experimentally analyzed, but its nominal values, based on the components used, are shown in Table 1.

### 2.2. Process Parameters

All experiments were performed with a frequency of 4.5 Hz. The starting procedure was conducted with solid slag and 3 g of Al-granulate for initial deoxidation. The process was started by so called “cold start procedure”. Therefore, the electrode was contacted with the Al-granulate and the baseplate, forming an open arc. Soon afterwards granulated solid slag components were inserted into the mold. Subsequently, the arc not only melts the electrode but also the solid slag and the system changes from arc heating to resistance heating. During the initial arc phase the Al-granulate act as a deoxidant. The whole slag is melted after typically 15 min. The parameters were selected to realize comparable melt rates, which required the adjustment of the melting current. The voltage was the result of an almost constant immersion depth of the electrode of about 0.5 to 1 cm. The main parameters of the remelting experiments are summarized in Table 2. No deoxidants were added to the slag during remelting. The ingot length after remelting was between 420 and 490 mm.

### 2.3. Materials Investigation

After remelting, the ingots were forged to a diameter of 60–80 mm. The forging started at a temperature of 1150 °C, was

**Table 1.** Nominal chemical compositions of the applied slags.

Trial, Slag	CaF <sub>2</sub> [wt%]	CaO [wt%]	Al <sub>2</sub> O <sub>3</sub> [wt%]	SiO <sub>2</sub> [wt%]	MgO [wt%]
3C3A	31.5	29.5	33.5	1.5	3
3C3A-N2	31.5	29.5	33.5	1.5	3
3C3A1S	29	27	30.5	10	3
4C4A	14.5	37.5	41.5	1.5	4
3A	68	-	30	2	-

**Table 2.** Process parameters of the remelting experiments.

Trial, Slag	Atmosphere	Slag [kg]	Current [kA]	Voltage [V]	Melt rate [kg h <sup>-1</sup> ]	Immersion [cm]
3C3A	air	5	3.5	60–62	63	1
3C3A-N2	N <sub>2</sub>	5	3.0	61–62	50	0.5
3C3A1S	air	5	2.9	74–75	51	1
4C4A	air	5	2.8	65–67	62	0.5
3A	air	6	4.0	60–63	57	0.5

conducted in one heat and completed above 900 °C. The degree of deformation  $A_{\text{initial}}/A_{\text{end}}$  was always between 4 and 7. Samples for chemical analysis and investigations on NMI were taken from the upper third of the forged ingot. Additionally, the slag was analyzed after remelting. An scanning electron microscope (SEM) JEOL JSM 6490 fitted with an Oxford Instruments X-Max 50 X-ray energy dispersive detector (EDX) and the AZtec Feature software suite was used for the automated analysis of the non-metallic inclusions. The system equips a W-emitter and the analyses were performed at an electron beam energy of 15 keV. The automated NMI scans were acquired in standardized fields of approximately 150 mm<sup>2</sup> using the backscattered electron signal. In this imaging mode NMI appear darker as the surrounding steel matrix due to the lower atomic number of NMI-typical elements such as O and S. This phase contrast allows the NMI to be recognized and their composition subsequently analyzed by EDX. With this method it is thus possible to fully characterize the position, size and composition of any inclusion located within the limits of the preset scan area. A detailed description of this method, its advantages and limits can be found in ref. [24]. All detected NMI with an oxygen content of 5 wt% or more and an S:O-ratio of <0.15 were considered oxides. Inclusions with oxygen and sulfur contents of at least 2 wt% each and an S:O-ratio between 0.15 and 6.67 were categorized as oxisulfides (conglomerates of oxides and sulfides). NMI with a sulfur content of 2 wt% or more and an O:S-ratio of <0.15 were taken as sulfides.

### 3. Results

#### 3.1. Chemical Composition of the Ingots

The chemical composition of the electrode and the remelted ingots is summarized in **Table 3**. There were no significant changes in the contents of C, Mn, Cr, Mo, and V due to the

remelting process. The chemical composition of the ingot remelted with the standard slag 3C3A lead to a significant reduction of the Si-content and a corresponding increase of the Al-content (**Figure 1**). The application of a protective nitrogen atmosphere has only a small impact on this reaction, leading to a slightly lower loss of silicon. By increasing the initial SiO<sub>2</sub>-content of this slag to 10% (3C3A1S) the Si-losses were reduced. Furthermore, the Al-content of the ingot remained almost constant compared to the electrode.

A variation of the CaF<sub>2</sub>-content toward lower CaF<sub>2</sub>- and higher CaO-, as well as Al<sub>2</sub>O<sub>3</sub>-contents (slag 4C4A) has only little effect on the chemical composition in comparison to the slag 3C3A. In contrast, remelting with slag 3A does not alter the Al-content compared to the electrode, despite having a similar Al<sub>2</sub>O<sub>3</sub>-content as slag 3C3A. Concerning the Si-content the use of slag 3A results in a similar reduction as the other low SiO<sub>2</sub>-containing slags.

The oxygen content after remelting was slightly reduced to 8–12 ppm at all experiments, except for remelting with the slag 3A, where the oxygen content almost doubled to 24 ppm. As expected for ESR-remelting, the sulfur content was reduced significantly from 13 ppm in the electrode to 4–9 ppm. The highest value was found for remelting with the slag 3C3A under protective N<sub>2</sub>-atmosphere.

#### 3.2. Chemical Composition of the Slag after Remelting

Changes in the SiO<sub>2</sub>- and the FeO-content are clear indicators for chemical reactions taking place during the remelting process. **Table 4** shows the slag composition after remelting for all five experiments. Open remelting with the slags 3C3A, 4C4A, and 3A results in a 2% to 3% increase in SiO<sub>2</sub> compared to the nominal starting composition and a FeO-content in the range of 0.1–0.2%. By using a protective nitrogen atmosphere, the gain of SiO<sub>2</sub> is reduced substantially and the final FeO-content was

**Table 3.** Chemical compositions of the electrode and the remelted ingots.

Trial, Slag	C	Si [wt%]	Mn [wt%]	Cr [wt%]	Mo [wt%]	V [wt%]	Al [wt%]	S [ppm]	O [ppm]
Electrode	0.36	0.95	0.4	4.8	1.2	0.4	0.018	13	13
3C3A	0.36	0.90	0.4	4.9	1.2	0.4	0.059	4	11
3C3A-N2	0.36	0.91	0.4	4.9	1.2	0.4	0.065	9	11
3C3A1S	0.36	0.93	0.4	4.9	1.2	0.4	0.015	6	12
4C4A	0.36	0.91	0.4	4.9	1.2	0.4	0.053	4	8
3A	0.36	0.91	0.4	4.9	1.2	0.4	0.016	8	24

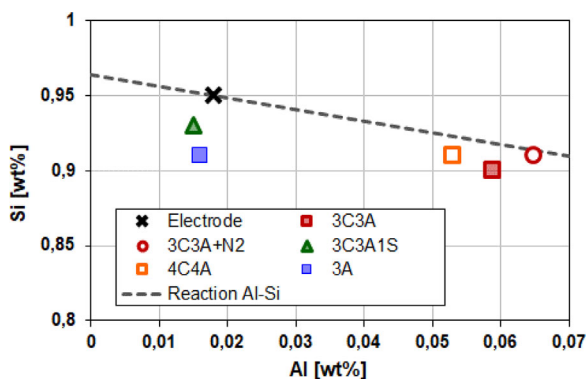


**Figure 1.** Silicon and aluminum contents in the electrode and after remelting.

below 0.05%. Adding 10% SiO<sub>2</sub> to the slag (3C3A1S) is effective in reducing the rise of the SiO<sub>2</sub>-content, but results in the highest FeO-level of all experiments.

Alterations of the other slag components were of minor importance and within the typical uncertainty of measurement, except for slag 3A. In the case of slag 3A, the Al<sub>2</sub>O<sub>3</sub>-content of the slag after remelting was only 23%. This can mainly be attributed to the high Al<sub>2</sub>O<sub>3</sub>-content in the slag skin at the copper mold, which leads to a continuous loss of Al<sub>2</sub>O<sub>3</sub> from the top-slag.

### 3.3. Non-Metallic Inclusions

#### 3.3.1. Content and Types of Non-Metallic Inclusions

**Figure 2** gives an overview on the total content (area%) of all types and sizes of non-metallic inclusions. Starting from the electrode, which contains mainly oxisulfides, but also noteworthy amounts of oxides and sulfides, remelting with the slags 3C3A (under air and under protective gas) and 3C3A1S leads to an increase of the pure oxides and a corresponding reduction of oxisulfides. While the total amount of NMI is slightly lower for remelting under protective nitrogen atmosphere, the addition of 10% SiO<sub>2</sub> does not have a significant effect on the total share of NMI. Pure sulfides were removed almost completely at all three remelting conditions.

The best results, especially regarding oxides, were found after remelting with the slag 4C4A, which also corresponds well with the lowest oxygen content of all ingots. In contrast, remelting with the slag 3A leads to a high content of NMI in total, especially

oxides, but to an extremely low content of oxisulfides. Again, the oxygen content corresponds well with the amount of oxides.

This picture changes significantly when only inclusions larger 5 μm are taken into consideration (**Figure 3**). All five remelted ingots have a significantly lower total content of NMI > 5 μm than the electrode. This is mainly based on the strong reduction of oxisulfides, combined with a moderate increase in oxides. Only the ingot remelted under the high SiO<sub>2</sub>-containing slag 3C3A1S has a noticeable high oxide content and some pure sulfides. After remelting with the slag 3A, the results for NMI > 5 μm are almost opposite to the results for all NMI. The share of oxides is on the same level as for the other slags and the total amount of NMI is the lowest.

#### 3.3.2. Size Distribution of Non-Metallic Inclusions

**Figure 4a–c** provide a more detailed information on the size distribution of the NMI. The number of oxides shrinks by several orders of magnitude with rising equivalent circle diameter (ECD), thereby the number of oxides in the ingots is higher than in the electrode for almost all sizes (**Figure 4a**). Up to an ECD of 5 μm, the highest amount of oxides was found after remelting with slag 3A.

In contrast, this slag lead to the lowest amount of oxisulfides by far (**Figure 4b**). As for the other remelted ingots, the number of small oxisulfides (< 5 μm) was similar to the electrode. The remelting process reduced larger oxisulfides significantly. With the exception of two large sulfides after remelting with slag 3C3A1S (**Figure 4c**), the amount of sulfides was reduced by one order of magnitude or more in all remelting trials and for all ECDs.

#### 3.3.3. Distribution of the Chemical Composition of Non-Metallic Inclusions

The chemical composition of the non-metallic inclusions is illustrated in the ternary system Al<sub>2</sub>O<sub>3</sub>–MgO–CaO in **Figure 5**, toward most of the inclusions could be assigned to. Therefore, all oxides and the oxidic parts of the oxisulfides were considered for evaluation. The analyzed compositions were projected to 100% by keeping their measured shares of Al<sub>2</sub>O<sub>3</sub>-, MgO-, and CaO-contents. White areas represent compositions where no NMI were detected. Blue areas correspond with those chemical compositions that were found only in low concentrations. In contrast, red areas show the chemical compositions with a large

**Table 4.** Chemical compositions of the slags after remelting.

Trial, Slag	CaF <sub>2</sub> [wt%]	CaO [wt%]	Al <sub>2</sub> O <sub>3</sub> [wt%]	SiO <sub>2</sub> [wt%]	MgO [wt%]	FeO [wt%]
3C3A	34.1	26.1	32.5	4.4	2.8	0.2
3C3A-N <sub>2</sub>	30.0	33.8	31.6	2.4	2.0	<0.05
3C3A1S	29.8	24.8	31.7	10.6	2.5	0.3
4C4A	12.8	36.6	41.9	4.8	3.5	0.15
3A	69.1	2.6	22.9	4.0	0.25	0.1

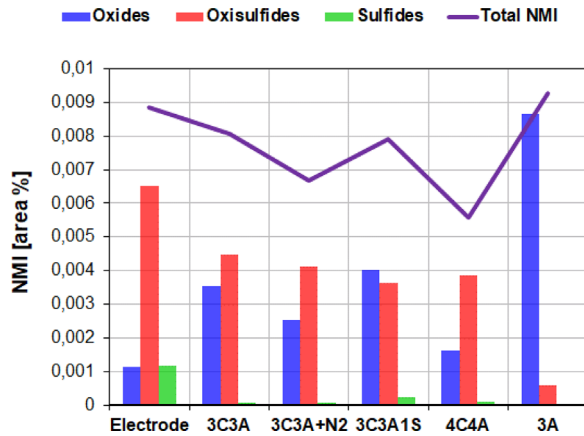


Figure 2. Content of non-metallic inclusion (NMI).

share of the total inclusion area. These concentrations are always based on the total content of NMI for each individual analysis and are not related to an absolute value. As the number of sulfides after remelting was very low, no detailed analysis of the sulfide composition was performed.

The main types of NMI in the electrode are  $MgO \cdot Al_2O_3$ - (MA-) spinel type as well as high MgO containing inclusions. A third group with a higher share of the total area of inclusions are pure  $Al_2O_3$ -type. Furthermore, some calcium–magnesia–aluminates with a wide area of chemical compositions were found. Remelting with the standard slag 3C3A leads to a concentration of the NMI in the area of the MA-spinel and some calcium–magnesia–aluminates with typically 50%  $Al_2O_3$  or more. Similar results were found after remelting under protective  $N_2$ -atmosphere and with the slag 4C4A, where the spinel-type inclusions were shifted toward higher MgO-contents and several high MgO containing inclusions were found, too.

The higher  $SiO_2$ -content of the slag 3C3A1S shifts the concentration of the MA-spinel as well as the calcium–magnesia–aluminates toward higher  $Al_2O_3$ -contents. Not visible in these figures, is another effect of the higher  $SiO_2$ -content in the slag. According to results published in ref. [9] especially calcium–magnesia–aluminates have higher  $SiO_2$ -contents with values of over 20%. High MgO-containing inclusions were also found in this sample.

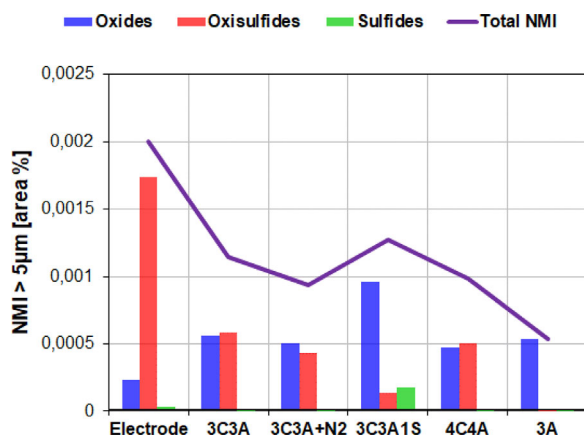
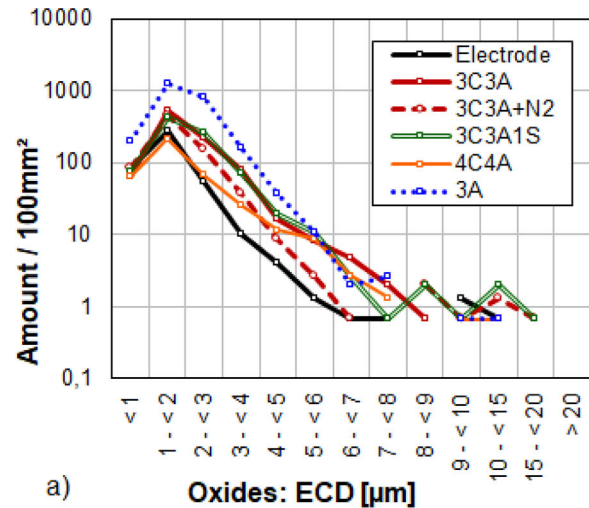
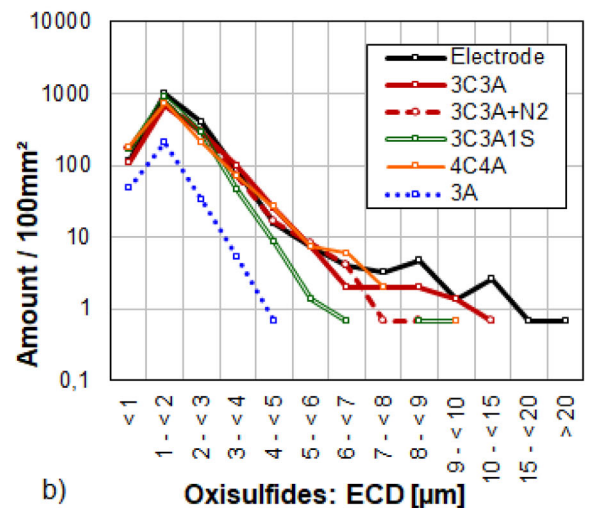


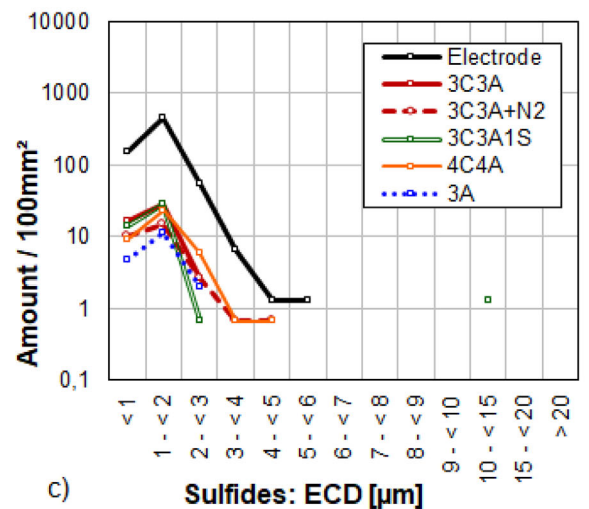
Figure 3. Content of non-metallic inclusion (NMI) > 5 μm.



a) Oxides: ECD [μm]



b) Oxisulfides: ECD [μm]



c) Sulfides: ECD [μm]

Figure 4. Size distribution by ECD of a) oxides, b) oxisulfides, c) sulfides.

In contrast to all these results are the compositions of the non-metallic inclusions after remelting with the CaO- and MgO-free slag 3A. Almost all of the detected NMI have high  $Al_2O_3$ -concentrations with minor contents of MgO or CaO.

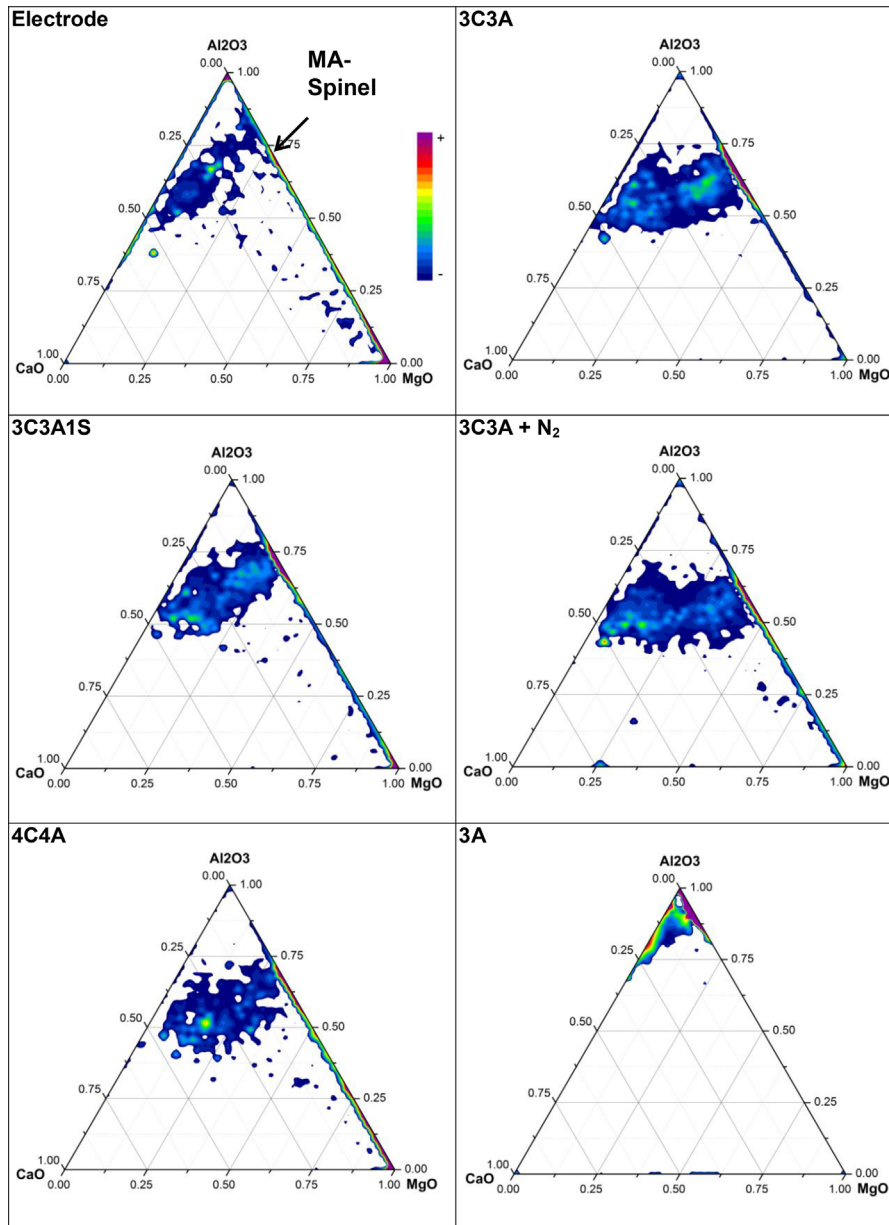
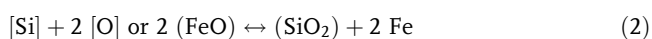
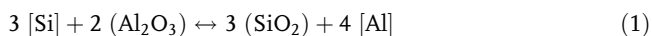


Figure 5. Chemical composition of the detected nonmetallic inclusion, density function according to the share in area.

## 4. Discussion

### 4.1. Chemical Reactions and Changes in the Composition of Steel and Slag

The loss of silicon and the gain of aluminum in the steel, according to refs. [1,2,8–10,25], depends largely on chemical reactions according to equation (1) and (2).



Thereby, Equation (1) describes the equilibrium between Si and Al in the steel and the content (activity) of  $\text{SiO}_2$  and  $\text{Al}_2\text{O}_3$  in the slag. This equilibrium condition is the primary reason for the reduced Si- and the increased Al-contents after remelting with the slags 3C3A and 4C4A and also for the reduced Si-losses and the low Al-content after remelting with the slag 3C3A1S. In the latter case, the higher  $\text{SiO}_2$ -content in the initial slag largely prevents reaction (1) due to an increase of the  $\text{SiO}_2$  activity in the slag. This corresponds with results in refs. [1,11] where the basicity  $\text{CaO}/\text{SiO}_2$  was used to describe the effect of higher  $\text{SiO}_2$  contents. The dashed line in Figure 1 indicates the stoichiometry according to Equation (1), which was (within analytical accuracy) fully observed only in the case of remelting under protective atmosphere. All other trials show a loss in total Al + Si and are

therefore situated below the equilibrium line due to oxidation effects.

As described in refs. [5,18], scaling of iron to iron oxide at the electrode surface above the slag, according to Equation (3), is the main source of oxygen uptake into the slag when remelting is performed without protective atmosphere.



Reaction (2) describes the subsequent effect of this FeO-uptake into the slag, leading to an additional loss of silicon (and aluminum). Both reaction (2) and (3) according to ref. [8] also contribute to the observed increase on SiO<sub>2</sub> and FeO in the slag as can be taken from Table 4. Therefore, using a protective atmosphere during remelting reduces the Si-losses and avoids the uptake of SiO<sub>2</sub> and FeO in the slag almost completely.

It is more difficult to understand the reactions for remelting with slag 3A. First of all, the loss of Al<sub>2</sub>O<sub>3</sub> in the slag from initially 30% to about 23% during remelting, in accordance with ref. [25], was proven to be the effect of preferential solidification of Al<sub>2</sub>O<sub>3</sub> in the slag skin at the ingot surface and has, therefore, nothing to do with potential chemical reactions between the melt and the slag. The Al-content in the remelted ingot is therefore also the same as in the electrode. The loss of Si into the slag (SiO<sub>2</sub>) and the rising FeO-content match well with those of the slags 3C3A and 4C4A. These changes can therefore be solely attributed to reaction (2) and (3). At similar contents of Si and Al in the electrode and SiO<sub>2</sub> in the slag after remelting, the reason why reaction (1) does not lead to an uptake of Al can only be explained by a significant increase of the Al<sub>2</sub>O<sub>3</sub>-activity, despite a reduced Al<sub>2</sub>O<sub>3</sub>-content. This correlates with Al<sub>2</sub>O<sub>3</sub>-activity data in ref. [26] proving that higher Al<sub>2</sub>O<sub>3</sub>-activities can be effective at significantly lower Al<sub>2</sub>O<sub>3</sub>-contents.

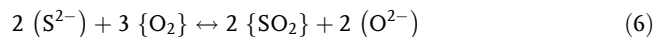
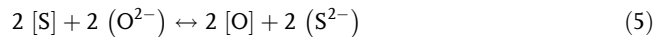
In difference to ref. [5], where the oxygen content was largely reduced by ESR, the oxygen level was lowered only slightly with all CaO rich slags despite no deoxidants were added during remelting. The explanation for this effect may be found in the already very low initial oxygen content of the electrode. The trend also matches with results in ref. [16] but on a lower oxygen level. Furthermore, the result from the higher SiO<sub>2</sub>-containing slag (3C3A1S) confirmed findings in ref. [9] that such additions of SiO<sub>2</sub> do not affect the oxygen content negatively.

Surprisingly the O-content after remelting with the dominantly Al<sub>2</sub>O<sub>3</sub>-containing slag 3A almost doubled but correlates well with findings in ref. [18], where a slag of type 3A lead also to higher O-contents than a CaO-containing multi-component slag. Taking into consideration the explanation given before on a higher Al<sub>2</sub>O<sub>3</sub> activity for this slag, the reactions according to Equation (4) will automatically lead to higher oxygen contents in the steel.



Changes in the sulfur content show significant desulfurization in all remelting trials, which is in agreements with the expected process behavior according to, e.g.<sup>[1,18,27]</sup> Nevertheless, the initial sulfur content is already very low, therefore differences in the final sulfur contents are more or less within the typical scatter of the analytical method. However, the highest sulfur

content was measured after remelting under protective atmosphere. According to refs. [1,18], this can be explained by the missing effect of slag renewal due to an oxidation of sulfur in the slag in contact with oxygen from the atmosphere according to Equation (5) and (6).



If the protective gas prevents reaction (6), reaction (5) leads to a continuous uptake in sulfur into the slag, reducing the capability for further desulfurization.

#### 4.2. Amount, Size, and Composition of NMI

All remelting trials led to significant reductions in sulfides and oxisulfides as well as to a more or less pronounced increase in oxides. The reduction in sulfides and oxisulfides is directly related to the reduction of sulfur as described before. This effect can also be held responsible for the increase in oxides as, according to findings in refs. [5,8,12], oxides often act as nucleus for the sulfide formation leading to mixed NMI, which is less relevant at such low sulfur contents.

The reduction of NMI is more pronounced for larger NMI, which is in good agreement with the expected behavior. The increase in fine oxide inclusions compared to the electrode corresponds to findings in ref. [16]. However the total amount of inclusions is significantly reduced, especially inclusions larger than 5 μm. Severe reductions of small inclusions (<2 μm) as reported in ref. [18] are probably the results of unspecified "microscopic observations".

The chemical compositions of NMI after remelting with the slag 3C3A (with and without protective atmosphere) are in good agreement with results from industrial production as described in ref. [15] with a majority of NMI in the area of the MA-spinel and also correlate broadly with results in refs. [9,14,16,18,20] despite information on the slag composition is partially missing. Variation of the slag compositions from roughly 30% CaO and Al<sub>2</sub>O<sub>3</sub> to 40% each as in slag 4C4A have only little effect on the composition of NMI except for an increased amount of high MgO inclusions, which corresponds with a slightly higher MgO-content of this slag. A positive effect of higher CaF<sub>2</sub>-contents on inclusion removal as described in ref. [28] for a Ni-base Superalloy could therefore not be confirmed. Higher SiO<sub>2</sub>-contents in the slag affect the SiO<sub>2</sub>-ration in the non-metallic inclusions significantly, which is described in detail in ref. [17] and correlates with earlier findings in refs. [1,9].

Removing CaO and MgO almost completely from the initial slag, as in case of slag 3A, changes the composition of NMI dramatically. Thereby alumina, in agreement with refs. [7,18], becomes the predominant type and the amount, especially of small oxide inclusions, more than doubled compared to the other remelted ingots. The explanation for this difference can be taken from the almost doubled oxygen content. As aluminum is the dominant deoxidant, reacting to more stable oxides than silicon and being significantly more available in the melt than

magnesium or calcium,  $\text{Al}_2\text{O}_3$  is preferentially formed during the cooling and solidification of the metal. The low MgO-content in the slag fosters this behavior. More oxides, due to the higher oxygen content, might also be the reason for the lower amount of oxisulfides, as the NMI-cluster may fall below the S:O-ratio threshold applied for the categorization.

This change in the composition of NMI with a complete removal of MA-spinel type inclusions is in contrast to findings in refs. [13,14], where this type on inclusions is assumed to have partially survived from the electrode. Thereby it has to be taken into consideration that investigations in refs. [13,14] focused on larger inclusions ( $>8\ \mu\text{m}$ ) with a more than 40 times wider area of detection. In this study the main content of inclusions is  $<8\ \mu\text{m}$  and can be regarded as newly formed during solidification. Therefore their composition is mainly based on equilibrium condition between aluminum and oxygen in the steel and not a question of survival from the electrode. This confirms findings in ref. [5] that the dominant part of oxygen in the steel can be found in small inclusions. These small inclusions cannot be removed into the slag by floatation in the liquid melt pool and become trapped in the advancing solidification front.<sup>[5,7,8]</sup>

## 5. Summary and Conclusions

Based on these results the following conclusions can be drawn.  
Chemical reactions:

- 1) The reactions between Si and Al in the melt and  $\text{SiO}_2$  and  $\text{Al}_2\text{O}_3$  in the slag follow the equilibrium condition.
- 2) Higher  $\text{SiO}_2$ -contents in the slag (3C3A1S) as well as a reduction of the  $\text{Al}_2\text{O}_3$  activity (slag 3A) can prevent the loss of Si and the subsequent increase in Al.
- 3) Except for remelting under protective atmosphere, all remelting trials showed a loss of Si + Al mainly based on FeO uptake to the slag by the oxidation of the electrode.
- 4) Open ESR also leads to higher FeO- and  $\text{SiO}_2$ -contents in the slag than remelting under protective atmosphere.
- 5) Sulfur was reduced despite an already very low initial sulfur level in the electrode, this effect was less pronounced under protective atmosphere.
- 6) The oxygen content after remelting was slightly lower than in the electrode except for the initially CaO- and MgO-free slag (3A), where the oxygen content almost doubled.
- 7) This increase in oxygen with slag 3A can be explained by an increase in  $\text{Al}_2\text{O}_3$ -activity.

Non-metallic inclusions:

- 8) The total content of non-metallic inclusions was reduced by ESR, except for remelting with the initially CaO- and MgO-free slag 3A.
- 9) Inclusions larger  $5\ \mu\text{m}$  were removed even more significantly with all slags.
- 10) While the content of oxides rose, oxisulfides were reduced and sulfides even stronger.
- 11) Therefore, the main improvement in cleanliness is based on the reduction of sulfur (removal of sulfides) as well as on the elimination of larger NMI.

- 12) Similar to the NMI-composition of the electrode, the highest content of NMI after remelting was of the MA-spinel type, except for the initially CaO- and MgO-free slag 3A.
- 13) Remelting with the initially CaO- and MgO-free slag 3A leads to  $\text{Al}_2\text{O}_3$ -type inclusions in the steel.
- 14) Higher MgO-contents in the slag result in more high-MgO containing NMI after remelting.

## Acknowledgements

The authors wish to thank voestalpine Böhler Edelstahl GmbH&CoKG for the financial, personnel and intellectual support. Likewise, the financial support of the Austrian Research Promotion Agency (FFG) for the "Competence Center for Excellent Technologies in Advanced Metallurgical and Environmental Process Development" (K1-Met) within the frame of the COMET-program is gratefully acknowledged. The article was modified after first online publication.

## Conflict of Interest

The authors declare no conflict of interest.

## Keywords

chemical reactions, electro-slag remelting, non-metallic inclusions, slag composition

Received: March 23, 2018  
Published online: July 5, 2018

- [1] W. Holzgruber, E. Plöckinger, *Stahl Eisen* **1968**, *88*, 638.
- [2] W. Holzgruber, E. Plöckinger, *Berg- Huettenmaenn. Monatsh.* **1968**, *113*, 83.
- [3] E. Plöckinger, *J. Iron Steel Inst.* **1973**, *211*, 533.
- [4] A. Mitchell, *J. Mater. Sci. Eng. A* **2005**, *413-414*, 10.
- [5] C.-B. Shi, X.-C. Chen, H.-J. Guo, Z.-J. Zhu, H. Ren, *Steel Res. Int.* **2012**, *83*, 472.
- [6] C. K. Mills, B. J. Keene, *Int. Met. Rev.* **1981**, *1*, 21.
- [7] A. Mitchell, *Ironmaking Steelmaking* **1974**, *1*, 172.
- [8] A. Mitchell, F.-R. Carmona, C.-H. Wei, *Iron Steelmaker* **1982**, *9*, 37.
- [9] M. Allibert, J. F. Wadier, A. Mitchell, *Ironmaking Steelmaking* **1978**, *5*, 211.
- [10] S. Radwitz, H. Scholz, B. Friedrich, H. Franz, in *Proc. Int. Symp. Liq. Met. Process. Cast.*, 2015 (Eds: A. Kharicha, M. Ward, H. Holzgruber, M. Wu), ASM International, Leoben, Austria, **2015**, 1.
- [11] H. Miska, M. Wahlster, *Arch. Eisenhuettenwes.* **1973**, *44*, 19.
- [12] J. Korp, *Berg- Huettenmaenn. Monatsh.* **2012**, *157*, 174.
- [13] E. Sjöqvist Persson, A. Mitchell, in *Proc. Int. Symp. Liq. Met. Process. Cast.*, 2017 (Eds: M. J. M. Krane, R. M. Ward, S. Rudoler, A. J. Elliott, A. Patel), TMS, Philadelphia, USA **2017**, 373.
- [14] E. Sjöqvist Persson, A. Karasev, P. Jönsson, in *Proc. Int. Symp. Liq. Met. Process. Cast.*, 2017 (Eds: M. J. M. Krane, R. M. Ward, S. Rudoler, A. J. Elliott, A. Patel), TMS, Philadelphia, USA **2017**, 353.
- [15] G. Reiter, W. Schuetzenhoefer, A. Tazreiter, C. Martinez, P. Wuerzinger, C. Loecker, in *Proc. Int. Symp. Liq. Met. Process. Cast.*, 2013 (Eds: M. J. M. Krane, A. Jardy, R. L. Williamson, J. J. Beaman), TMS, Austin, USA **2013**, 213.

- [16] J.-H. Liu, G.-X. Wang, Y.-P. Bao, Y. Yang, W. Yao, X.-N. Cui, *J. Iron Steel Res. Int.* **2012**, 19, 1.
- [17] R. Schneider, C. Schüller, P. Würzinger, G. Reiter, C. Martinez, *Berg-Huettenmaenn. Monatsh.* **2015**, 160, 117.
- [18] Y.-W. Dong, Z.-H. Jiang, Y.-L. Cao, A. Yu, D. Hou, *Metall. Mater. Trans. B* **2014**, 45, 1315.
- [19] R. Schneider, M. Müllleder, P. Zeller, P. Würzinger, G. Reiter, S. Paul, *Berg- Huettenmaenn. Monatsh.* **2016**, 161, 20.
- [20] A. Paar, R. Schneider, P. Zeller, G. Reiter, S. Paul, I. Siller, P. Würzinger, *Steel Res. Int.* **2014**, 85, 570.
- [21] R. Schneider, M. Molnar, C. Schüller, S. Gelder, G. Reiter, C. Martinez, in *TOOL 2016, Proc. of 10<sup>th</sup> Int. TOOL Conference – TOOL 2016* (Ed: F. Simancik) ASMET, Bratislava, Slovakia **2016**, 303.
- [22] R. Schneider, M. Molnar, C. Schüller, S. Gelder, G. Reiter, C. Martinez, in *Proceedings of IFM 2017–20th International Forgemasters Meeting 2017* (Ed: B. Buchmayr), ASMET, Graz, Austria **2017**, 326.
- [23] R. Schneider, A. Paar, P. Zeller, G. Reiter, W. Schützenhöfer, P. Würzinger, *Berg- Huettenmaenn. Monatsh.* **2011**, 156, 112.
- [24] R. Werl, G. Klösch, W. Winkler, A. Pissenberger, M. W. Egger, S. Aigner, J. Pühringer, S. Michelic, C. Bernhard, W. Schützenhöfer, R. Schneider, C. Schüller, *Berg Hüttenmaenn. Monatsh.* **2012**, 157, 194.
- [25] A. Mitchell, *Can. Metall. Q.* **1981**, 20, 101.
- [26] M. Hino, S. Kinoshita, H. Ito, S. Yorozuya, *CAMP-ISIJ* **1994**, 7, 41.
- [27] H. Miska, M. Wahlster, *Arch. Eisenhuettenwes.* **1973**, 44, 81.
- [28] M. H. Manjili, M. Halali, *Metall. Mater. Trans. B* **2018**, 49, 61.